



## OPEN ACCESS

## EDITED BY

Frédéric Frappart,  
INRAE Nouvelle-Aquitaine Bordeaux, France

## REVIEWED BY

Cassandra Normandin,  
INRAE Nouvelle-Aquitaine Bordeaux, France  
Lijuan Song,  
Sun Yat-sen University, China

## \*CORRESPONDENCE

Jeremy Stoll,  
✉ Jeremy.Stoll@gmail.com

RECEIVED 29 May 2025

REVISED 24 December 2025

ACCEPTED 08 January 2026

PUBLISHED 26 January 2026

## CITATION

Stoll J, Jasinski M, Robbins J, Hancock D and Nattala J (2026) Real-time modulation of a global inland water body reference mask using ICESat-2 for identification of dynamic water surface extents.

*Front. Remote Sens.* 7:1637802.  
doi: 10.3389/frsen.2026.1637802

## COPYRIGHT

© 2026 Stoll, Jasinski, Robbins, Hancock and Nattala. This is an open-access article distributed under the terms of the [Creative Commons Attribution License \(CC BY\)](#). The use, distribution or reproduction in other forums is permitted, provided the original author(s) and the copyright owner(s) are credited and that the original publication in this journal is cited, in accordance with accepted academic practice. No use, distribution or reproduction is permitted which does not comply with these terms.

# Real-time modulation of a global inland water body reference mask using ICESat-2 for identification of dynamic water surface extents

Jeremy Stoll<sup>1,2\*</sup>, Michael Jasinski<sup>2</sup>, John Robbins<sup>3,4</sup>,  
David Hancock<sup>1</sup> and Jyothi Nattala<sup>1,5</sup>

<sup>1</sup>Science Systems and Applications, Inc., Lanham, MD, United States, <sup>2</sup>Hydrological Sciences Laboratory, Code 617, NASA Goddard Space Flight Center, Greenbelt, MD, United States, <sup>3</sup>Craig Technologies Inc., Merritt Island, FL, United States, <sup>4</sup>Cryospheric Sciences Laboratory, Code 615, NASA Goddard Space Flight Center, Greenbelt, MD, United States, <sup>5</sup>Terrestrial Information Systems Laboratory, Code 619, NASA Goddard Space Flight Center, Greenbelt, MD, United States

In order to take advantage of the unprecedented opportunity to measure global inland surface water heights using new-generation spaceborne instruments like ICESat-2's Advanced Topographic Laser Altimeter System (ATLAS), robust water body shape information is necessary to group photon returns into body transits for along-track processing and to define water edges. A code environment that is able to combine known water body extent from past studies with real-time satellite observations can allow for such results. Even a static water body mask representing the state of a previous time, when working in conjunction with dynamic width-finding software algorithms that take advantage of contemporary return analysis, offers the opportunity for analysis of water surface profiles that change between satellite overpasses. However, previously existing masks do not include all water body types, are of insufficient resolution, or are not native to a format that allows for precise buffering, scalability, and efficient file size. By merging diverse buffered data sets in a modular, updatable fashion, a new global inland water body masking approach is created that can work in conjunction with an operational retrieval algorithm to identify water bodies globally and process to their edges for ICESat-2 analysis or other scientific investigations.

## KEYWORDS

hydrology, ICESat-2, inland water, lakes, lidar, remote sensing, rivers

## 1 Introduction

Accurate measurements of inland water body height statistics have been limited in the past by many constraints, including the resources required for adequate *in situ* data acquisition, the technology available for airborne missions to meet the desire for ambitious spatial and temporal coverage, and seasonally unreliable water boundary masks of disparate body types, accuracy, and completeness. The emergence of Earth observing photon-counting lidar has enabled the successful study of global lake and river storages remotely (Busker et al., 2019; Tortini et al., 2020; Cooley et al., 2021) and provided opportunities for valuable long-term monitoring of water surface heights (Ricko et al., 2012; Birkett, 2010).

## 1.1 Purpose of the ATL13 inland water body shape mask

Although the recent advances in altimetry allow for the study of water bodies from edge to edge at higher frequency and resolution, the nature of continuous data collection on orbit presents the obvious need for the algorithmic inclusion of a water boundary mask to allow for the isolation, organization, and analysis of the photon returns by unique body during processing of raw returns. Previous efforts to define terrestrial water extent focused on statistical estimations of surface area (Lvovich, 1970; Downing et al., 2006), constructed static water body datasets unable to account for the dynamics of seasonal or long-term boundary changes (Verpoorter et al., 2014; Messenger et al., 2016), or produced large catalogs of temporal water extent datasets not feasible to ingest for operational production of a continuous global inland water product (Biswas et al., 2019). On their own, these types of boundary masks do not meet the need for a global solution that includes a variety of body types and can be merged with operational edge-finding software to take advantage of high-resolution data provided by frequent overpass of evolving water body boundaries. The construction of a fully-featured dataset of static water boundaries, partnered operationally with a dedicated processing algorithm designed to take advantage of the reference information it provides, creates a software environment that enables accurate global output, edge-finding flexibility, and operational efficiency for lidar-based inland water products (Jasinski et al., 2023).

To take advantage of the opportunity provided specifically by multi-track lidar like ICESat-2 for high-resolution products over inland water, an innovative coupling of an inland water body mask to the processing flow is desirable for a number of reasons. By designing a data production algorithm to operate on a photon-by-photon basis, it can take advantage of precise body edges and incorporate them into its processing chain for anomaly identification and edge detection, both of which are critical to computing the initial coarse water body height upon which the algorithm relies. Through comparison of the intersection range of retrieved photons and a reference mask, the algorithm can operate efficiently on inland water features, grouping product output by individual body for easy access by the user, and not wasting computation on photons outside the inland water domain. With a mask that includes attribute information for each shape, bodies of different types and sizes can be handled in customized fashions through buffering operational control parameters that accommodate the changing width of lakes and rivers, which might, for example, provide instructions to search for braids in a river but not in a bay. Thus, even static mask input can be utilized as a guide by which customized production software can be given a processing domain and then rely on its own techniques for finding water edges at a specific time of satellite overpass that does not coincide with the time of the reference mask input's boundary capture. By creating a high-resolution mask that includes all types of bodies in a mission domain, the product is optimized for accuracy, operational efficiency, and user-friendly output format. Rather than requiring access to a swath of masks of different formats, creation of a single mask

reduces processing effort and improves accuracy for altimetry analysis or any science requiring reliable, flexible water body boundaries that allows software to examine dynamic edges falling inside or outside a reference edge.

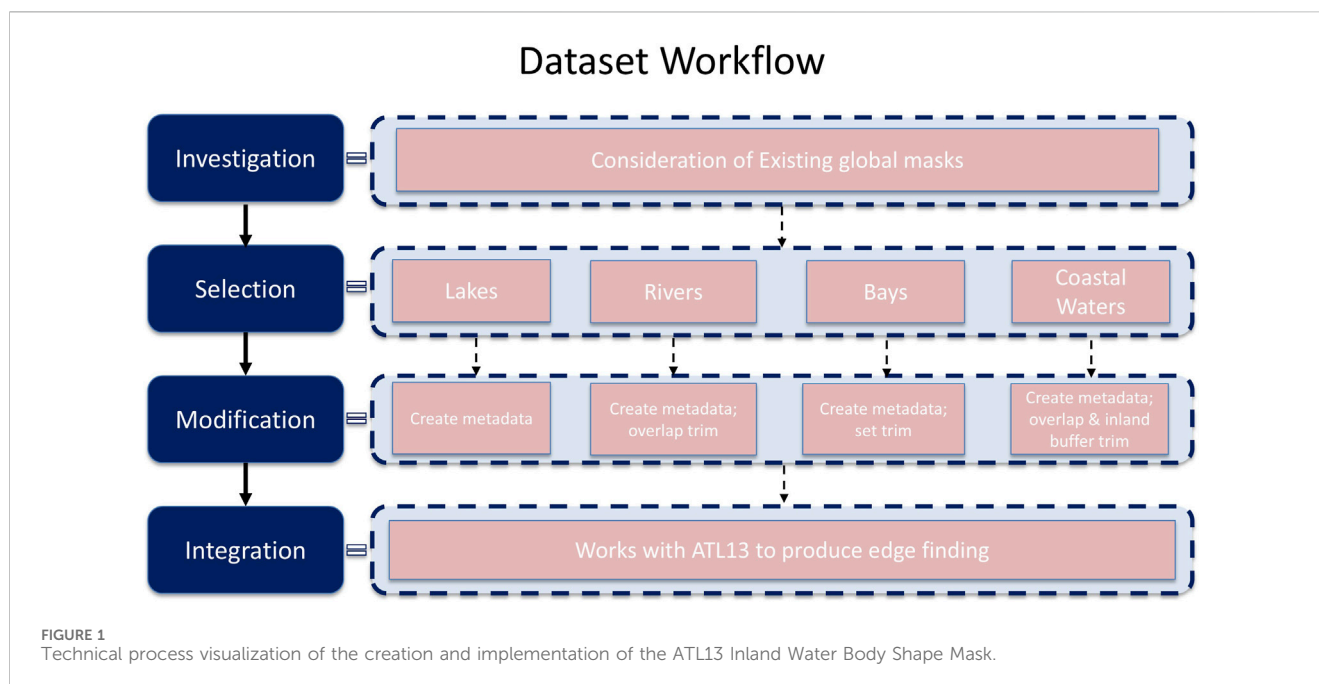
## 1.2 ICESat-2 ATLAS mission

NASA's ATLAS instrument, launched aboard ICESat-2 in September 2018, is a 532 nm photon-counting instrument with a near polar orbit (92°) inclination angle capable of surveying 17-m footprints observed every approximately 70 cm (10 Hz) along track. ATLAS is configured with six beams, aligned as three pairs each spaced 3 km apart, with 30 m between weak and strong paired beams orbiting at a 91-day repeat (Markus et al., 2017). Although the repeat tracks are exact over the polar regions, mid-latitude ground tracks off-point approximately 29 km in each repeat cycle, allowing for the mapping of vegetation over time while also capturing data over a larger number and variety of lakes than exact repeats would provide. This configuration is optimized for ice sheets and sea ice – the mission's primary targets – but also allows for computation of other altimetry-based data products that include oceans, land, atmosphere, and inland water. Even prior to launch, the value of this type of data to hydrology was demonstrated through the ICESat-2 Early Adopter program (Brown et al., 2016) and study of the ICESat-2 airborne prototype Multiple Altimeter Beam Experimental Lidar (Jasinski et al., 2016). ICESat-2 has operated successfully in the period since launch (Martino et al., 2019) and is already producing important results regarding inland waters (Zhang et al., 2019; Li et al., 2019; Yuan et al., 2020; Ma et al., 2020; Ryan et al., 2020). These results highlight the successful implementation of a global, flexible composite mask of lakes and width-based river estimates (Pavelsky et al., 2008) developed for high-resolution repeat patterns of the ICESat-2 inland water data product.

Higher level ICESat-2 data products, including the Along Track Inland Surface Water Data product, rely on the Global Geolocated Photon Data (ATL03) dataset to provide input height, geolocation, signal classification, quality, necessary geophysical corrections, and uncertainty of each photon collected by the instrument detectors as well as indicators of the degree of background noise, saturation, or first photon bias within the instrument pulse that generated the photon at approximately 20-m increments, defined by ATL03 as a geosegment (Neumann et al., 2019). Such high-resolution horizontal and vertical data provide a valuable opportunity, when processed in a code environment that provides water body reference boundaries that are able to be dynamically adjusted based on real-time observations by intentionally-designed software, to find water body heights and edges down to the highest resolution units of output for a product like ATL13.

## 2 Methods

The inland water body mask works in conjunction with high-resolution ATL03 photon-rate input into the ATL13 processing code to identify a water body, define its extent, and calculate its statistics. In order to match the needs of the algorithm design and the requirements of the product, the mask must consist of:



- Global coverage of lakes, rivers, bays, and coastal waters, as defined in scope and size by the ATL13 ATBD (Jasinski et al., 2023);
- Vector formatting to allow for precise buffering and investigation around a shape edge, flexible scalability, and efficient data file size;
- Robust attribute definition allowing for identification and differentiation between lakes, reservoirs, rivers, and bays, as well as the estimation of river characteristics through width and braiding definition;
- Spatial resolution significantly finer than ICESat-2 geosegment-rate definition, nominally 20 m, used to consider a photon for inclusion in processing.

The achievement detailed by this Technical Note includes all aspects of the Inland Water Body Shape Mask, from creation out of source datasets to integration with the operational software (Figure 1). This description must include the investigation, selection, modification, and integration of the datasets utilized to create it.

## 2.1 Investigation: consideration of existing masks and datasets

Before construction of a new shape mask, an examination of existing masks in the literature was performed to assess whether their coverage and resolution were sufficient to meet the goals of ATL13. The algorithm requires that a mask must include lakes, rivers, bays, and global coastal waters, and inversely requires that ocean beyond the coastal zone must be excluded. Typical high-resolution digital elevation models, even products that take care to integrate water boundary information into their construction, are of limited utility in identifying lake or shore boundaries susceptible to seasonal and annual variation (Robinson et al., 2014), which puts global coverage at odds with high shape-level resolution.

The Terra Moderate Resolution Imaging Spectroradiometer (MODIS) Land Water Mask (MOD44W) based on the Shuttle Radar Topography Mission (SRTM) complimentary SRTM Water Body Data (SWBD) coastline product (Carroll et al., 2009), which provides global coverage at 250-m resolution, is not sufficient when operating on 0.1 square kilometer lakes in ATL13 processing, for which the algorithm attempts to identify water body edges on less than a 25-m basis. Other masks provide higher resolution but less robust global coverage or do not include certain body types, such as the 30-m pixel resolution The Terra Advanced Spaceborne Thermal Emission and Reflection Radiometer (ASTER) Global Water Bodies Database (ASTWBD) that was created as part of the ASTER Global Digital Elevation Model (ASTER GDEM) product (Abrams et al., 2020), which lacks the body type attributes of which the algorithm could take advantage, and does not differentiate among multiple water bodies in close proximity.

Global water extent products like the Global Surface Water Explorer (GSWE) (Jean-François et al., 2017) and the Surface Water and Ocean Topography mission (SWOT) (Pavelsky et al., 2014) provide valuable data at a spatial and temporal resolution that merit consideration for use in the ATL13 mask aggregation. However, due to operational constraints of ATL13 production, ongoing ingest of datasets as they are made available is not a tenable solution, nor a necessary one in the desired framework of dynamic software edge finding. So, while these types of datasets are valuable for temporal and seasonal change study of water extent (Aires et al., 2018; Bonassies et al., 2026), in this investigation they are most useful as validation ICESat-2 ATL13 results.

A number of regional masks exist, mostly the results of focused efforts to serve particular areas (Hess et al., 2012; Yan et al., 2019), industries (U.S. Fish and Wildlife Service, 2019), or scientific purpose (Falcone et al., 2017). Although the attention and insight afforded to local studies most often leads to a high-quality product, a patchwork approach to global coverage using these types of granular datasets of disparate resolutions and format is not likely to maintain resolution during combination, nor achieve global coverage.

TABLE 1 Selected input sources to the ATL13 Inland Water Body Shape Mask (v3).

ATL13 inland water body shape mask (v3) input		
Body type	Count	Source
Lakes & Reservoirs	18 (Area $\geq 10,000$ km <sup>2</sup> )	HydroLAKES (Messenger et al., 2016)
	160 (10,000 > A $\geq 1,000$ )	
	1,530 (1,000 > A $\geq 100$ )	
	14,981 (100 > A $\geq 10$ )	
	168,492 (10 > A $\geq 1$ )	
	1,242,507 (1 > A $\geq 0.1$ )	
Rivers	10,253	Global River Widths from Landsat (GRWL) (Allen and Pavelsky, 2018a)
Coastal Waters	11,297	The Global, Self-consistent, Hierarchical, High-resolution Geography (GSHHG) Database (Wessel and Smith, 1996)
Bays	188	Named Marine Water Bodies (NMWB) (Esri, 2016)
Total Shapes	1,449,426	

The existing data sets that were considered, while useful for other purposes, do not meet the operational needs and product requirements of high resolution ATL13 processing design. This fact presented an opportunity to instead seek out recent high-resolution data sets for each type of body, customize attributes for algorithm inclusion, and aggregate a new mask for ATL13 from a variety of sources. Rather than relying on a single source, the ATL13 Inland Water Body Shape Mask was constructed from various inputs best-suited to the data regime of ICESat-2, allowing for the inclusion of various body types and able to be updated in a segmented approach as improved inputs emerge. The result is a mask of consistent format that reduces the effort required to buffer edges prior to processing, instead allowing operational software to examine a customized distance inside or outside the reference boundaries to identify changing water extent, as defined algorithm parameters.

## 2.2 Selection: aggregation of datasets

The ICESat-2 ATL13 Inland Water Body Shape Mask was developed after considering existing shape data over lakes, rivers, estuaries, bays, and coastlines when selecting input components (Table 1). Water body boundaries change frequently, which is difficult to capture without expanding the database beyond a reasonable processing size, but recent versions of data can better represent those boundary changes that are more stable over the future of near-term missions. The nature of the mask aggregation allows for piecemeal data set replacement in the future when justified by resolution at any spatial coverage, rather than requiring the need to wait for an improved global product before an update can be made.

### 2.2.1 Lakes and reservoirs

Earth's largest lakes, those with an area greater than 500 square kilometers, are present on all continents except Antarctica (Herdendorf, 1982). However, when considering all lakes greater than 0.1 square kilometers for ATL13 analysis, only 9 percent of

lakes exceed an area of one square kilometer (Downing et al., 2006). Most of these smaller lakes are found in the higher latitudes of the Northern hemisphere, coincident with the denser crossings of ICESat-2, where the bulk of the planet's lake to shore interface exists (Winslow et al., 2014). Therefore, due to the high resolution ATL03 photon availability and high frequency of measurement to capture temporal changes, a lake input to the inland water body mask that includes lakes as small as 0.1 square kilometer provides ideal global coverage of lakes with sufficient crossing lengths to be processed through the ATL13 segment-based algorithm at all latitudes.

Although Landsat is a proven tool for mapping water extent (Pickens et al., 2020), high-resolution tile maps based on Landsat scenes such as the Global 1-s Water Body Map (G1WBM) (Yamazaki et al., 2015) present processing challenges to convert from raster format to individual lake shapes with discrete attributes and boundaries at questionable upscaling resolution, and one-arcsecond resolution is insufficient for mapping cases with lakes in near proximity to one another. The Global Lakes and Wetlands Database (Lehner and Döll, 2004) includes the desired set of lake sizes and shape attributes, although its inventory is lacking in small lakes and is based on boundaries that are now decades old. The earliest versions of the ATL13 mask utilized GLWD for its lake polygon input (Jasinski et al., 2019), taking advantage of the various sources that went into its creation and the global coverage of various lake sizes that it offered.

In order to achieve higher resolution and add more robust global coverage of small lakes, HydroLAKES (Messenger et al., 2016) was introduced to recent versions of the ATL13 mask, increasing the ATL13 lake shape count by over five hundred percent. HydroLAKES incorporated well-established localized sources such as Canadian CanVec and the Alaskan NHD to build on GLWD, achieving resolution as high as 30-m boundary definition in those areas. Primarily based on SWBD in the mid-latitudes, the HydroLAKES data set presents strong global coverage supported by regional products updates in key areas of ICESat-2 inland water domain while allowing the ATL13 algorithm to produce water heights,

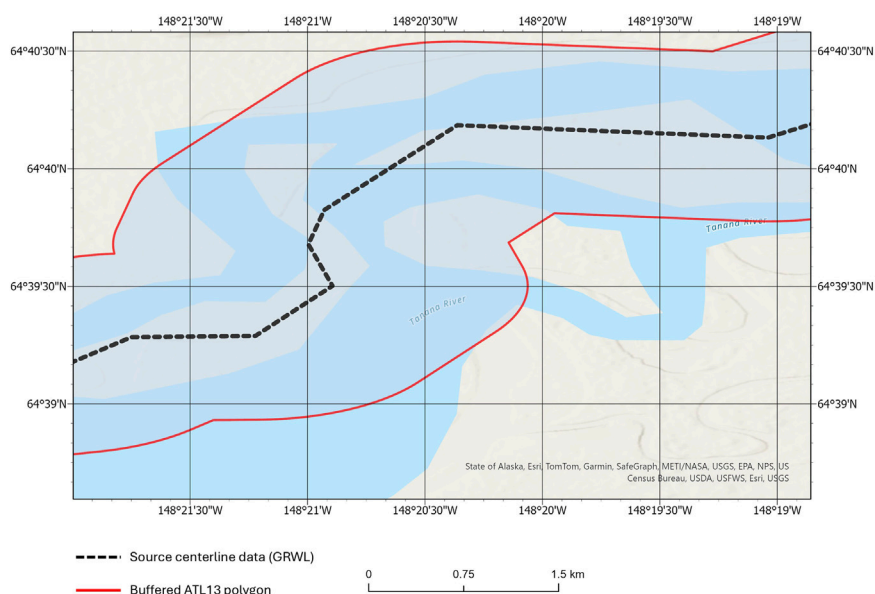


**FIGURE 2**  
Tanana River near Fairbanks, Alaska, as represented in the ATL13 Inland Water Body Shape Mask. Buffered centerline source data ensures inclusion of all braids and edges within the processing domain, allowing the software algorithm to determine boundaries based on lidar returns observed at the time of overpass (basemap credit (Esri and DigitalGlobe, 2025)).

statistics, and edges over 1.4 million lakes. Incorporation of smaller lakes included in the SWOT Prior Lakes Database (Wang et al., 2023) and improved availability of high meter-scale resolution commercial datasets including Planet and Maxar may lead to even further refined masking in the future.

### 2.2.2 Rivers

Rivers present a unique challenge for inclusion in the ATL13 mask as most available data sets are in the form of centerline polylines and width regimes, representing rivers in discrete segments while at the same time not grouping the data into intuitive river networks. The requirement of the ATL13 algorithm design to utilize polygonal data requires that width attributes be present in any river polyline dataset to transform the lines into polygonal shapes that can bound a set of lidar photon returns. Although typical static river width data might represent an average flow condition rather than extreme, that width can be used to buffer the polyline to the extent that confidence can be high that most states of flow will be within the resulting boundary used during ATL13 processing.

Although well-designed for continental-scale basin study and including a high count of rivers, the HydroRIVERS catalog (Lehner and Grill, 2013) does not provide a width with its segments, while Esri's World Linear Water product (Esri, 2025) has an insufficient shape count to supply to ATL13 and also lacks river width attributes. The Merit HYDRO global river data set was also considered (Yamazaki et al., 2019), however its width resolution, raster format, and lack of accounting for river braiding do not meet the requirements of a serviceable mask to the ATL13 algorithm.

For inclusion in the most recent version of the ATL13 body mask, the Global River Widths from Landsat (GRWL) Database (Allen and Pavelsky, 2018a) was selected for several reasons,

including proven success determining river characteristics from Landsat (Allen et al., 2020). The river coverage and count in the summary statistic version of the product meet the needs and capabilities of ATL13 to process river crossings, and the shapes are accompanied by a robust attribute set that includes minimum, maximum, median and mean widths by which to extrapolate into polygons from the centerlines, and those widths account for full width across braids along with a braiding index (Allen and Pavelsky, 2018b). Although the dataset does not provide specific definition for varying flow extent and multichannel rivers, it allows GIS software to translate the centerlines into shapes for overpass analysis, giving operational ATL13 processing a reliable domain over which to detect more precise edges. After testing various configurations for inclusion in the current version of the ATL13 mask, summary GRWL centerlines were buffered on each side by four times the width of median flow (Figure 2). This translation of centerlines to shapes resulted in two-thirds of river segment mask shapes equaling at least seventy-five percent of maximum flow source data, while exceeding twice the maximum flow in fewer than ten percent of segments. Although the latter cases will include significant amounts of land beyond the actual flow extent, operational software such as ATL13 intentionally designed to find water edges that do not align with a reference edge welcomes a processing domain that is too wide rather than too narrow to do its boundary investigation.

By incorporating buffered GRWL centerlines into the aggregate mask, a photon-counting analysis like ATL13 not only is well-positioned to produce accurate river surface statistics, but also to interface with altimetry results from SWOT47, which rely on a similar dataset for river definition in its Level 2 River Single-Pass

Vector Data Product (SWOTST, 2023) in studies that are already underway (Altenau et al., 2021).

### 2.2.3 Coastal waters

As previously described, the ATL13 Inland Water product includes surface statistics and bathymetry in the coastal zone, which is defined as ocean water within 7 km of continental or island coastline (Jasinski et al., 2023). In order to create shapes that capture the near-shore area of oceans and bays, a global coastline data set of high resolution was necessary, which then could be buffered from the coastline away from land using GIS software to create a global, polygonal dataset of the desired coastal water body extent.

High resolution coastline exists locally for places of interest like islands (Sayre et al., 2019), and as part of an ongoing mapping effort of the CoNED USGS project (Gesch et al., 2016), but piecing together global coverage from local efforts is not feasible. Openstreetmap land boundaries provide the coverage needed, though the nature of the updating of the set leads to concerns about uneven quality (Openstreetmap, 2025). The Global, Self-consistent, Hierarchical, High-resolution Geography (GSHHG) Database (Wessel and Smith, 1996), which includes continental and island coverage at approximately 40-m resolution in the full-resolution product meets the requirements of the algorithm design and was selected for inclusion in the ATL13 mask.

### 2.2.4 Bays

The ATL13 inland water domain also includes major bays not identified by the selected lake and reservoir input set or enclosed by coastline buffering, so it is necessary to append the ATL13 body mask to achieve this processing coverage. For this purpose, the Named Marine Water Bodies (Esri, 2016) data set was included in the mask, with all bodies greater than approximately 1.2 million square kilometers removed, preserving bodies as large as Hudson Bay in the set while excluding additional swaths of oceans and seas outside the inland water domain from entering ATL13 analysis.

## 2.3 Modification: aggregation and formatting of dataset components

Because the ATL13 algorithm is designed to process photons within a prescribed inland water domain, relying solely on static shapes in a mask with no opportunity for dynamic adjustments during operations presents risk that seasonal and annual boundary variations might not adequately be taken into consideration. In order to ensure capture of water body edges, along with some amount of land for the algorithm's edge-finding module to access, the ideal processing domain extends beyond the actual contemporaneous edges of the water body onto the land. This domain extent can best be accomplished by a combination of: (a) expanding the initialized mask extent by buffering the member shapes upon their inclusion in the mask, and (b) allowing operational software like that of ATL13 to create along-track buffered zones that trigger processing beyond the edges of the original shape when necessary or accommodate edges inside the mask when that situation occurs. In order to avoid excessive overlap of shapes in the data set and preserve the original extent for future

examination, the domain around lake and bay edges is slightly expanded using a buffer coded into the ATL13 software. This adjustment is implemented via a control parameter in the algorithm, instructing the processing of the water body to include some number of ATL03 geosegments outside the mask boundary for each feature processed. It is currently set to five geosegments for all water body types and sizes (Jasinski et al., 2023), taking advantage of the vector shapes to judiciously expand beyond instances of mask imperfections and seasonal variation while avoiding inclusion of enough land to corrupt the water surface calculations.

Data sets were merged in GIS software, preserving common shape attribute categories for population in the aggregate mask file. Due to the combining of disparately sourced data sets, overlapping shapes were produced in areas like river mouth outlets into bays, which were removed in after duplicate identification by assigning the overlapping area and attributes of an intersection to one of the participating shapes and removing the other in the set. The selection of which shape to award the allocation of intersecting area was implemented hierarchically as per the priorities of the ATL13 product, with any overlaps first becoming part of a collocated lake, then river, then bay that could make a claim to the shared area. In most circumstances, the overlap was either a river interrupted by a reservoir, or a coastal buffer encroaching inland onto a river, estuary, or bay. The result is a set of unique shapes with unique identifiers optimized for ICESat-2 inland water processing, but useful to any application where water boundary information is needed for the analysis of water or shore statistics.

In addition to the shapes and attributes that were derived based on selected inland water body shape data sets, a continental-scale basin map was used to identify to which basin each shape belongs. This regional map is based on aggregation of HydroSHEDS basin polygons (Lehner and Döll, 2004) into ten continental-scale shapes, and rather than requiring the import and consideration of large shapes in the algorithm flow, the basin ID is simply added to the shapefile attribute list for each water body as an integer. Any application of the inland water body shape mask could thus be filtered by continental location analysis and organization if a user desired.

## 2.4 Integration: operational interaction with the ATL13 algorithm

The ATL13 product algorithm environment, currently implemented at version 7, calculates inland surface water surface height, standard deviation, and other characteristics over bodies based on the photon heights retrieved by ATLAS and processed through ATL03 (Jasinski et al., 2023). Water bodies targeted for analysis include lakes greater in size than 0.1 square kilometer, rivers, estuaries, bays, and near-shore coastal zones. Output files generated by ATL13 processing are produced for every four ICESat-2 orbits, approximately 6 h of data, populated along-track at a short segment rate of nominally 100 signal photons, which are typically between 25 and 100 m in length and are allowed by operational code buffering parameters to fall within any distance on either side of a body mask reference boundary to account for seasonal change in storage and streamflow.

TABLE 2 Guide to interpreting the numerical identification assignment of an inland water body in the mask, processing flow, and product output.

ATL13refID formatting (TSCXXXXXXX)		
Body type (T)	Body area size (S), km <sup>2</sup>	Body cited source (C)
Lake (1)	Area > 10,000 (1)	HydroLAKES (Messenger et al., 2016) (1)
Reservoir (2)	10,000 > A ≥ 1,000 (2)	Global Lakes and Wetlands Database (Winslow et al., 2014) (2)
River (5)	1,000 > A ≥ 100 (3)	Named Marine Water Bodies (Sayre et al., 2019) (3)
Estuary/Bay (6)	100 > A ≥ 10 (4)	GSHHG Shoreline (Altenau et al., 2021) (4)
Coastal Zone (7)	10 > A ≥ 1 (5)	Global River Widths from Landsat (Lehner and Grill, 2013) (5)
	1 > A ≥ 0.1 (6)	
	Not Assigned, i.e., for rivers (9)	

XXXXXXX seven-digit unique body identifier for use when full suite of descriptors is not needed.

The integrity of the ATL13 Inland Water Body Shape Mask is critical to initially identifying individual water body crossings, their coarse surface heights, and eventually their edges. The boundaries provided by the mask to the software algorithm are relied on to define the processing domain over which anomalous heights can be found and discarded. First, by identification of all water surface photons within the mask and parameterized buffer distance, and then by computing the short segment along track height statistics assuming a Gaussian surface for each beam. The edges of the water surface or an interior land segment are then isolated and identified by eliminating those short segments with anomalous heights.

By considering the proximity of each photon return to the static boundaries provided by the mask and its height to the estimated water surface level, the system evolves into dynamic edge finding where photons may be identified as water boundaries in the processed product regardless of where they fall relative to the input mask reference boundary.

## 3 Result

### 3.1 Body count and composition

The ATL13 Inland Water Body Shape Mask is the result of merging of the collected different water body types and includes approximately 1.45 million body shapes aggregated from high-resolution sources of various types and sizes (Table 1). Lakes as small as 10 ha, major river systems, estuaries, bays, and global near-shore coastline are represented and made available to ATL13 for identification of ATL03 photons relevant to inland water processing.

### 3.2 Shape attributes and format

In order to provide consistent and efficient interfacing with any lidar-based inland water operational code such as ATL13, the mask was designed in a standard shapefile format, containing as much information in as few attributes as possible while still allowing room for waterbody count expansion. In addition to the body polygon itself, the operational code reads in only two attributes for each

shape to begin analysis. The primary attribute ingested is ATL13refID, a ten-digit number that includes the body type (T), size (S), source (C), and unique identifying number (X) in the format TSCXXXXXXX, as defined by the ATL13 Algorithm Theoretical Basis Document (Jasinski et al., 2023) (Table 2). Care was taken to ensure that the identifying number (X), even if it had been a duplicate within source data sets, is unique for every water body in the mask if trimmed away from the 3-digit prefix.

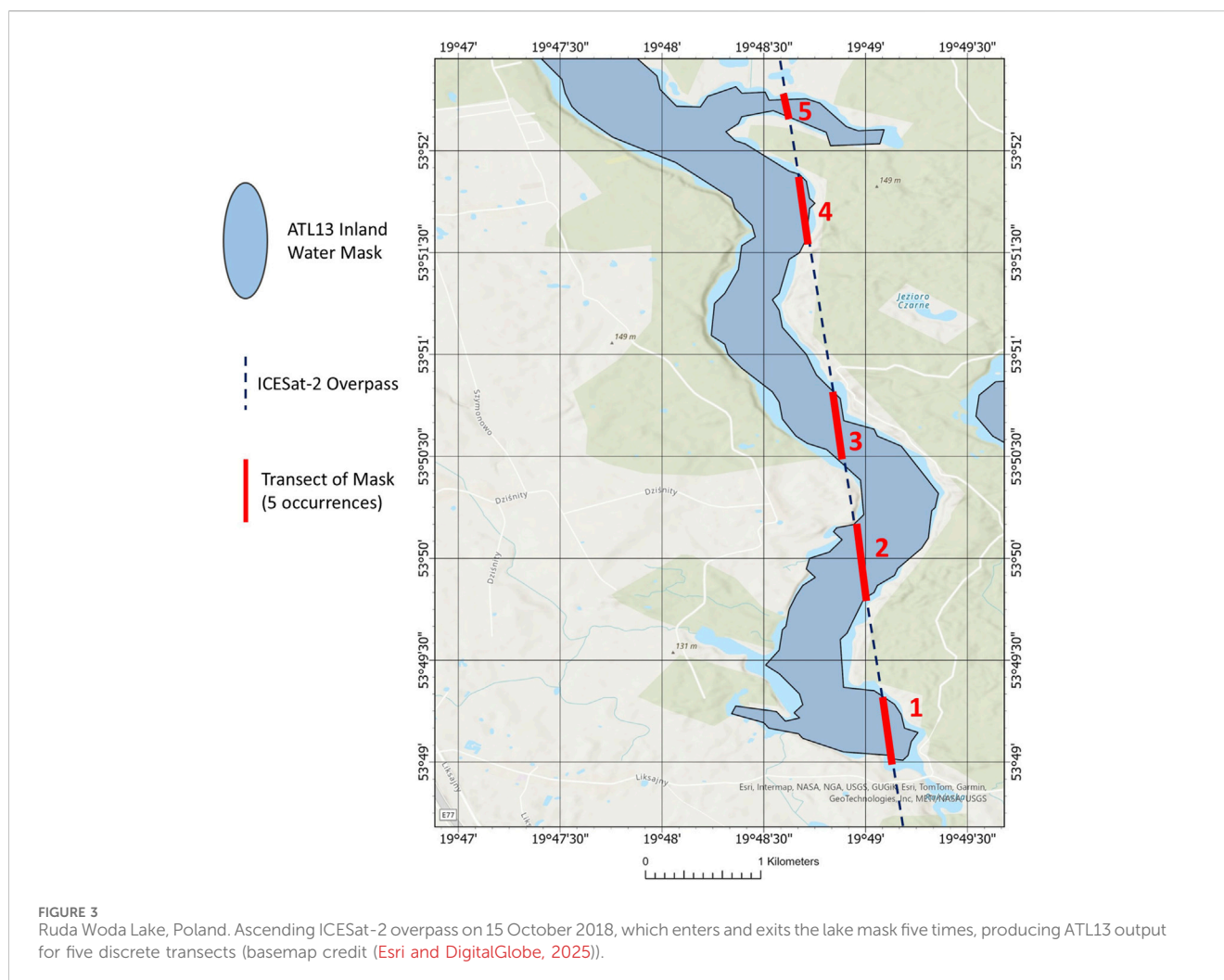
## 4 Discussion

The ATL13 Inland Water Body Shape Mask is utilized by the ATL13 operational code as an ancillary (ANC) file, allowing shapes and their attributes to be read in as necessary based on wherever on the globe relevant ATL03 input is located to eliminate unnecessary consideration of the entire set of photons for every water body calculation. As ATL03 provides geolocated data along track, the ATL13 Inland Water Body Shape Mask assists processing by: (a) eliminating the need to process photons outside the inland water domain, (b) providing an initial edge estimate, and (c) providing a framework by which to logically group output.

The ATL13 Inland Water Body Shape Mask provides additional processing tools by embedding water body type and size in ATL13refID. Control parameters are described in the ATBD which provide flexibility for the algorithm to be instructed to produce output for only certain water body types or sizes. The presence of this information also allows the algorithm to perform different operations on different body types and sizes if desired, allowing for different algorithm paths to processing Hudson Bay and a small river, rather than a one-size-fits-all approach.

### 4.1 Body transecting

The mask enables ATL13 output to be calculated and grouped not only by water body, but by discrete transects within the body when appropriate. For example, an ICESat-2 crossing that exits and reenters the mask due to a peninsula of land several times will be processed separately based on each entry and exit pair and



represented in the output by short segments with the same body ID but different transect IDs (Figure 3). By providing ATL13 a reference mask of the water body presenting the interruption of a crossing to operational software able to process smaller units within a body, long segment statistics can be isolated from any corruption caused by the inclusion of land.

## 4.2 Body edges

Although annual, seasonal, and more frequent boundary changes are certain to occur, the mask provides a coarse water reference edge from which to begin more refined analysis and can be dynamically buffered within software to capture water surface outside its bounds when imperfectly representing current conditions. In the case of Ruda Woda Lake, Poland during an 15 October 2018 ICESat-2 crossing, the static mask fell well short of the actual water boundaries, but the software was able to work with the static mask input and the photons it was receiving to determine accurate boundaries (Figure 4). Any short segment determined to be of sufficient height to be marked anomalous is excluded from standard processing of ATL13 inland water output, and is

instead included in a separate anomaly subgroup, and available in the ATL13 product for study in approximation of water edge down to the photon-level based on output across both groups.

Although not yet available globally for much overlap of the ICESat-2 mission period, the Landsat Level-3 Dynamic Surface Water Extent (DSWE) Science Product (Jones, 2019) offers an opportunity to examine the ATL13 results against the Landsat-derived body boundaries at the time of crossing. The water level of Lake Mead, Nevada has changed significantly since its capture into the HydroLAKES database that was included in the mask, but by pairing that static boundary with real-time analysis of photon heights in and around the mask edge, the ATL13 algorithm is able to successfully identify the domain of the water body on June 2022 crossing and limit the output to within the lake's actual extent during overpass (Figure 5).

While DSWE is only available in north America for use in comparison study, the SWOT Level 2 Water Mask Raster Image Data Product, Version C (Surface Water Ocean Topography SWOT, 2024) offers a global opportunity to validate water body edge finding with proven success (Wu et al., 2025). During an ICESat-2 overpass of Lake Annecy in the French Alps on 28 June 2023, the ATL13 Inland Water Body Mask results can be compared with

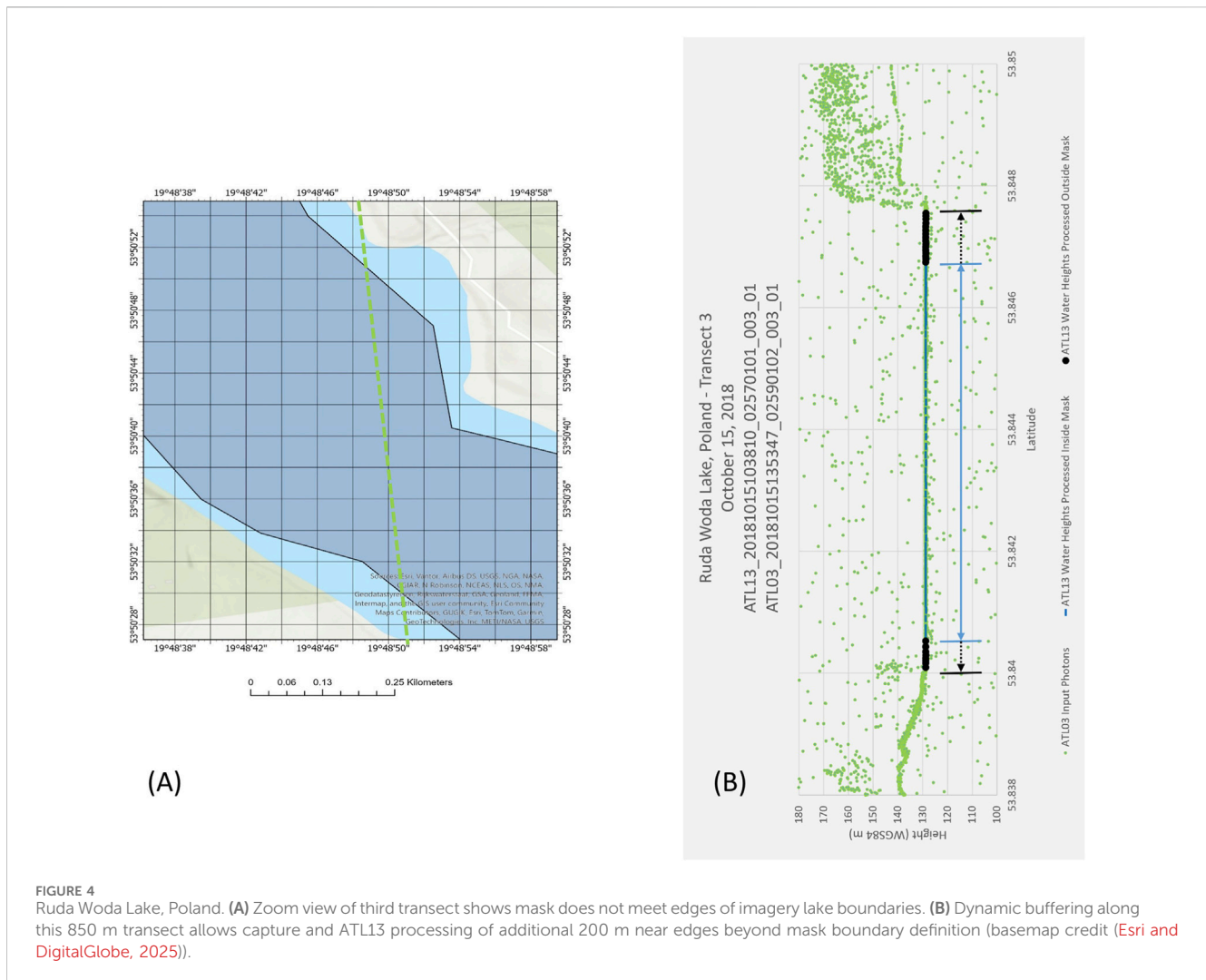


**FIGURE 4**  
Ruda Woda Lake, Poland. **(A)** Zoom view of third transect shows mask does not meet edges of imagery lake boundaries. **(B)** Dynamic buffering along this 850 m transect allows capture and ATL13 processing of additional 200 m near edges beyond mask boundary definition (basemap credit (Esri and DigitalGlobe, 2025)).

the extent observations of the SWOT L2 Lake Single-Pass Vector Obs Data Product (Figure 6). Unlike the Lake Mead case, this situation is one where the ATL13 mask falls short of the observed water instead of exceeding it. Once again, the software in tandem with the algorithm is able to process water around the margins of the static boundary to match observations.

### 4.3 Complex rivers

Although a static mask boundary inside a lake extent as it actually exists at the time of overpass is not problematic due to the edge being identifiable as the end of the continuous surface, a river presents a different problem due to frequent interruptions by land within the river or complex braiding. Seasonal river extent changes and more frequent fluctuations critical to flood assessment can be challenging to successfully monitor through photon-by-photon resolution afforded by lidar analysis. By extending the mask beyond the typical flow extent of most rivers, the ATL13 inland water algorithm is able to access the amount of data necessary to determine edges in any flow regime. As

demonstrated in the processing of a crossing of the Tanana River near Fairbanks, Alaska (Figure 7), where the mask extends well beyond the August 2022 flow extent, the algorithm uses at the ATL03 input to successfully find water edges inside the mask, even as the river is split into numerous individual channels due land interruptions. Despite the braided complexity of the river, dynamic buffering along this transect allows capture of adequate data as algorithm input to identify water heights and edges in the same channels as the DSWE scene.

### 4.4 Conclusions

Hydrological analysis of off-pointing lidar altimetry requires a boundary mask solution to take advantage of its sampling accuracy and organize processing efforts and output, while also able to interface with processing software in the determination of dynamic water body edges. Although the creation a water body mask meeting the requirements of ATL13 processing was the primary purpose for the effort, the resulting dataset and integrated operational coding approach has application beyond

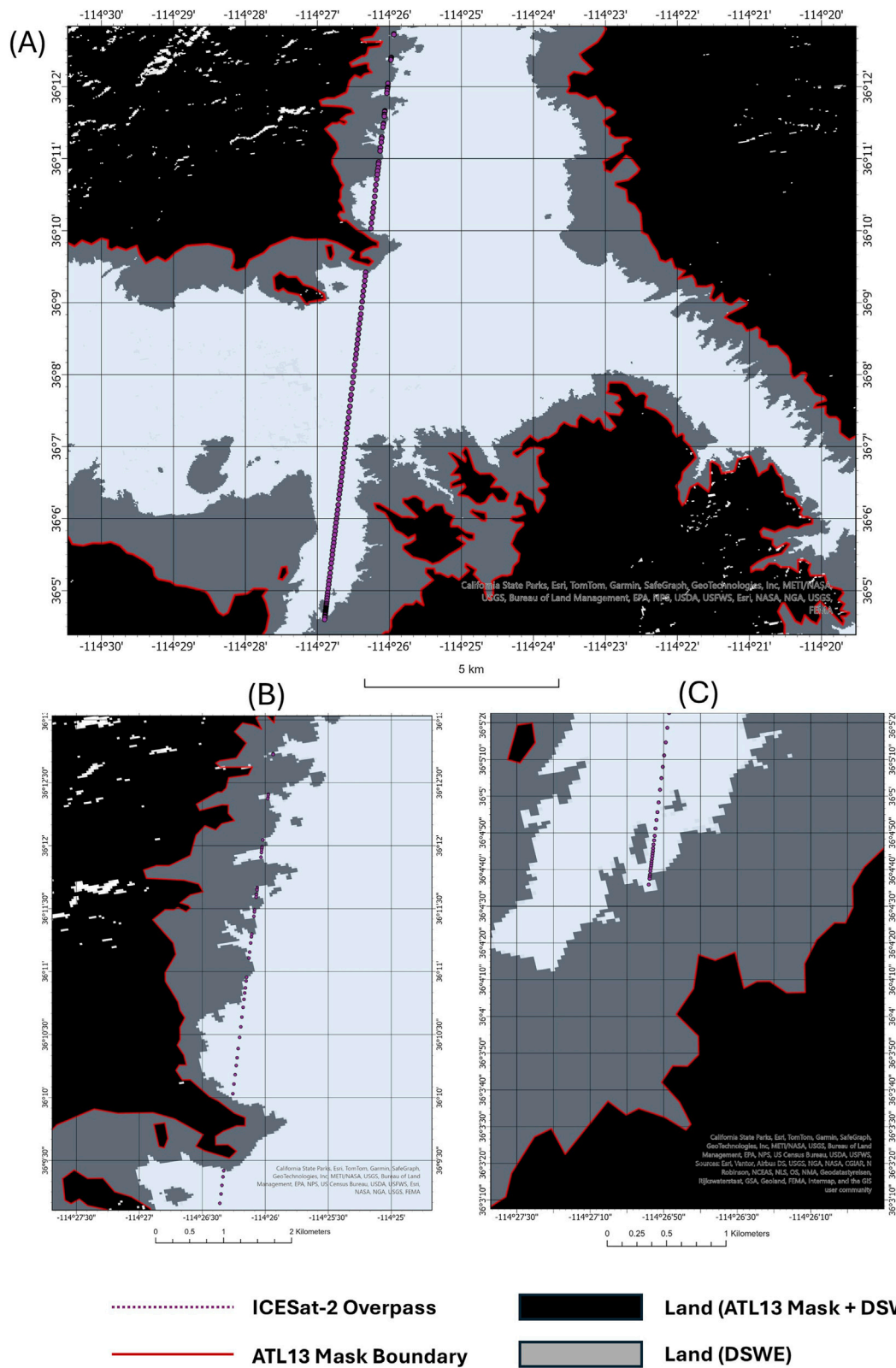
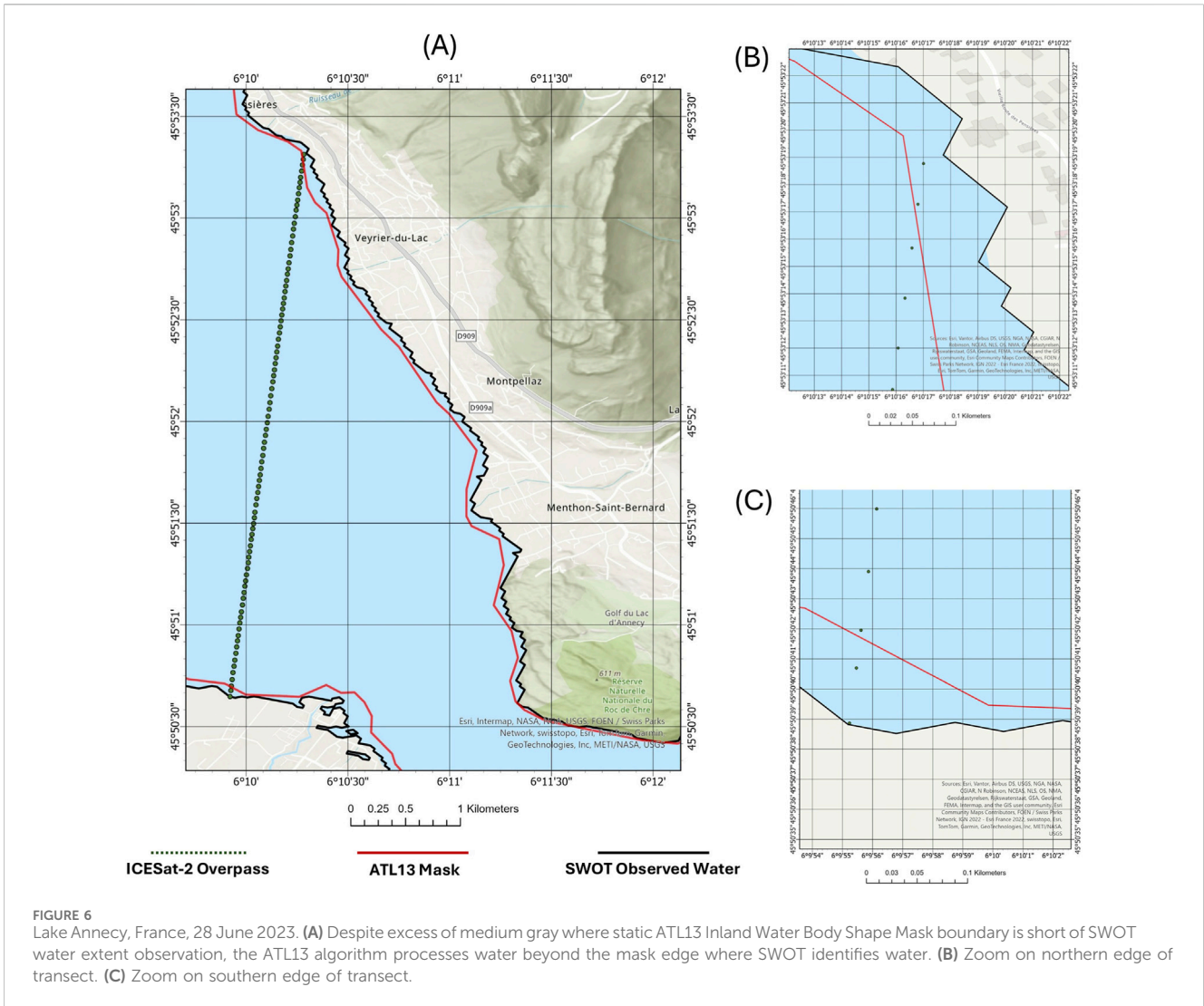


**FIGURE 5** Lake Mead, Nevada, United States, 11 June 2022. (A) Despite excess of masked land where ATL13 boundary exceeds DSWE water observations, the ATL13 algorithm finds water coincident only with where DSWE identifies water. (B) Zoom on northern edge of transect. (C) Zoom on southern edge of transect.

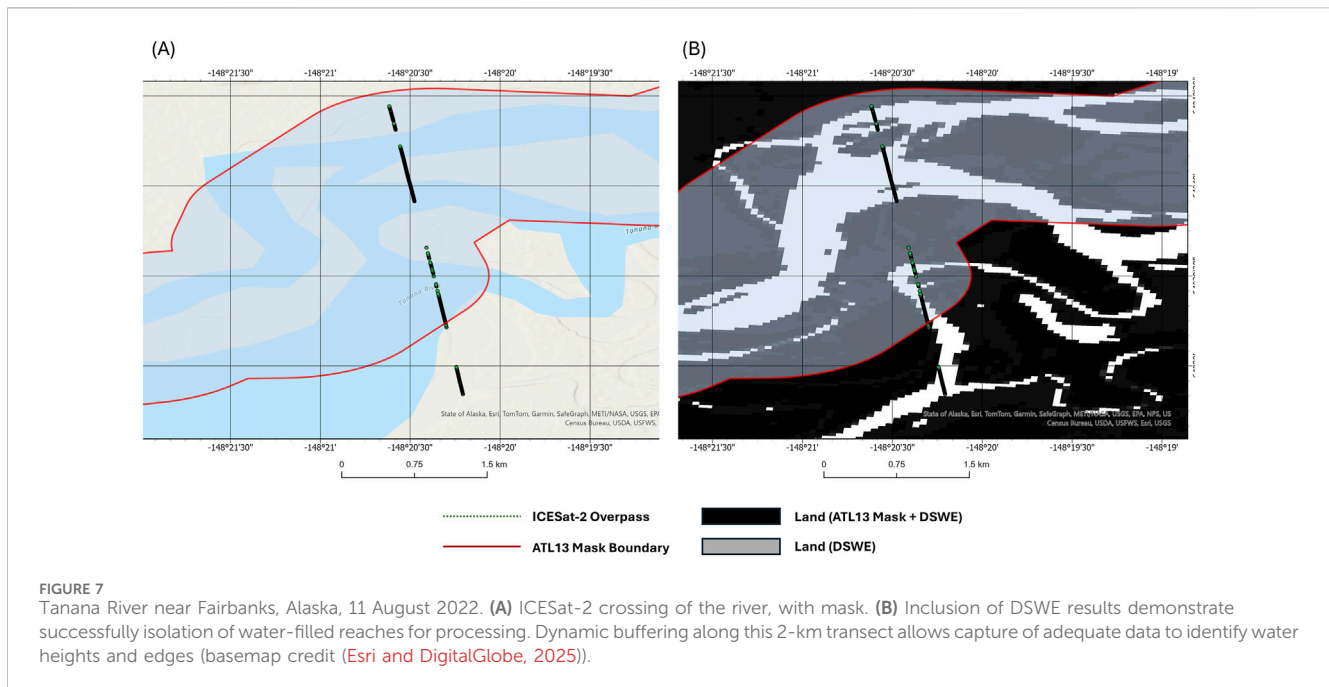


ICESat-2 science. By compiling disparate body boundary sources into a single dataset of shapes with common attributes and formatting, any application can benefit from the efficiency of a single file of vector boundaries that can be scaled in a customized fashion to mask more or less area than the native shape dimensions as desired. Additionally, by incorporating high-resolution, updated inputs to the mask, accuracy is not sacrificed for the benefit of simple interfacing with a single shapefile rather than multiple sets. When coupled with operational software that can iterate based on the nature of the input returns to analyze height domains in the effort to identify edges, the mask demonstrates success as a tool in the ICESat-2 analysis of seasonally variable water extent.

Despite its static nature, ATL13 Inland Water Body Shape Mask allows the ICESat-2 inland water operational code environment to function as designed, providing information needed to achieve key objectives. First, the mask allows ATL13 processing to avoid unnecessary computation outside of the domain of water body shapes, while also dynamically identifying surface outside the mask that is a candidate for inland water processing based on shape definition. Secondly, the high-resolution mask allows for a targeted search for water

body edges through the ATL13 height anomaly finding routine. Finally, it provides shape attribute information by which the ATL13 output can be organized by water body through the tagging of unique water body and transect identification. This allows for efficient and accurate inland water processing as well as easy access and manipulation of output data for a particular body of interest to an ICESat-2 user, provides a robust catalog of body shapes for any investigation requiring boundary information, and contributes to hydrologic science's progress to define water surface extent globally through efforts like the next-generation of DSWE, DSWx-HLS (Jet propulsion laboratory, 2025), being produced at a global scale (Zwally et al., 2002).

As ATL13 algorithm development has evolved, it has been necessary for the ATL13 Inland Water Body Shape Mask to match its ambition for high resolution processing of water bodies of various types and sizes. Mask updates are transparent to the operational code without issue or detriment of the algorithm's science objectives, demonstrating the feasibility of ingesting new boundary data as it becomes available while maintaining consistent formatting of the body mask.



## Data availability statement

The datasets presented in this study can be found in online repositories. The names of the repository/repository and accession number(s) can be found below: <https://nsidc.org/data/icesat-2>.

## Author contributions

JS: Writing – original draft, Formal Analysis, Methodology. MJ: Supervision, Writing – review and editing, Project administration, Methodology. JR: Resources, Writing – review and editing. DH: Software, Writing – review and editing. JN: Writing – review and editing, Software.

## Funding

The author(s) declared that financial support was received for this work and/or its publication. This work was supported by the ICESat-2 Project Office at NASA Goddard Space Flight Center and the NASA Cryosphere, Terrestrial Hydrology, and Physical Oceanography Programs.

## Acknowledgements

We gratefully acknowledge Jeffrey Lee, Claudia Carabajal, Charon Birkett, and Jeffrey Guerber, who provided valuable insight toward development of the ATL13 mask.

## Conflict of interest

Authors JS, DH, and JN were employed by Science Systems and Applications, Inc. Author JR was employed by Craig Technologies Inc.

The remaining author(s) declared that this work was conducted in the absence of any commercial or financial relationships that could be construed as a potential conflict of interest.

## Generative AI statement

The author(s) declared that generative AI was not used in the creation of this manuscript.

Any alternative text (alt text) provided alongside figures in this article has been generated by Frontiers with the support of artificial intelligence and reasonable efforts have been made to ensure accuracy, including review by the authors wherever possible. If you identify any issues, please contact us.

## Publisher's note

All claims expressed in this article are solely those of the authors and do not necessarily represent those of their affiliated organizations, or those of the publisher, the editors and the reviewers. Any product that may be evaluated in this article, or claim that may be made by its manufacturer, is not guaranteed or endorsed by the publisher.

## References

- Abrams, M., Crippen, R., and Fujisada, H. (2020). ASTER global digital elevation model (GDEM) and ASTER global water body dataset (ASTWBD). *Remote Sens.* 12, 1156. doi:10.3390/rs12071156
- Aires, F., Prigent, C., Fluet-Chouinard, E., Yamazaki, D., Papa, F., and Lehner, B. (2018). Comparison of visible and multi-satellite global inundation datasets at high-spatial resolution. *Remote Sens. Environ.* 216, 427–441. doi:10.1016/j.rse.2018.06.015
- Allen, G. H., and Pavelsky, T. M. (2018a). Global river widths from landsat (GRWL) database (version V01.01). *Zenodo*. doi:10.5281/zenodo.1297434
- Allen, G. H., and Pavelsky, T. M. (2018b). Global extent of Rivers and streams. *Science* 361, 585–588. doi:10.1126/science.aat0636
- Allen, G. H., Yang, X., Gardner, J., Holliman, J., David, C. H., and Ross, M. (2020). Timing of landsat overpasses effectively captures flow conditions of large Rivers. *Remote Sens.* 12, 1510. doi:10.3390/rs12091510
- Altenau, E. H., Pavelsky, T. M., Durand, M. T., Yang, X., Frasson, R. P. d. M., and Bendeu, L. (2021). The surface water and ocean topography (SWOT) mission river data base (SWORD): a global river network for satellite data products. *Water Resour. Res.* 57, e2021WR030054. doi:10.1029/2021wr030054
- Birkett, C. M. (2010). *From research to operation: the USDA global reservoir and Lake monitor*. Coastal altimetry. 1st ed. New York: Springer-Verlag, LLC.
- Biswas, N. K., Hossain, F., Bonnema, M., Okeowo, M. A., and Lee, H. (2019). An altimeter height extraction technique for dynamically changing rivers of South and South-East Asia. *Remote Sens. Environ.* 221, 24–37. doi:10.1016/j.rse.2018.10.033
- Bonassies, Q., Fatras, C., Peña Luque, S., Dubois, P., Piacentini, A., Cassan, L., et al. (2026). A comprehensive study of surface water and ocean topography (SWOT) pixel cloud data for flood extent extraction. *Remote Sens. Environ.* 333, 115101. doi:10.1016/j.rse.2025.115101
- Brown, M. E., Delgado Arias, S., Neumann, T., Jasinski, M. F., Posey, P. G., Babonis, G., et al. (2016). Applications for ICESat-2 data: from NASA's early adopter program. *IEEE Geoscience Remote Sens. Mag.* 4 (4), 24–37. doi:10.1109/MGRS.2016.2560759
- Busker, T., de Roo, A., Gelati, E., Schwatke, C., Adamovic, M., Bisselink, B., et al. (2019). A global lake and reservoir volume analysis using a surface water dataset and satellite altimetry. *Hydrology Earth Syst. Sci.* 23 (2), 669–690. doi:10.5194/hess-23-669-2019
- Carroll, M. L., Townshend, J. R., DiMiceli, C. M., Noojipady, P., and Sohlberg, R. A. (2009). A new global raster water mask at 250 m resolution. *Int. J. Digital Earth* 2 (4), 291–308. doi:10.1080/17538940902951401
- Cooley, S. W., Ryan, J. C., and Smith, L. C. (2021). Human alteration of global surface water storage variability. *Nature* 591 (7848), 78–81. doi:10.1038/s41586-021-03262-3
- Downing, J. A., Prairie, Y. T., Cole, J. J., Duarte, C. M., Tranvik, L. J., Striegl, R. G., et al. (2006). The global abundance and size distribution of lakes, ponds, and impoundments. *Limnol. Oceanogr.* 51, 2388–2397. doi:10.4319/lo.2006.51.5.2388
- Esri (2016). Named marine water bodies. Available online at: <http://mappingcenter.esri.com/index.cfm?fa=arcgisResources.gisData>.
- Esri (2025). World linear water provides a detailed basemap layer for the rivers, streams, and canals of the world. Available online at: <https://www.arcgis.com/home/item.html?id=273980c20bc74f94ac96c7892ec15aff>.
- EsriDigitalGlobe. (2025). IGN, IGP, swisstopo, and the GIS user community. ArcGIS basemap credit.
- Falcone, J. A., Baker, N. T., and Price, C. V. (2017). *Watershed boundaries for study sites of the U.S. geological survey surface water trends project*. U.S. VA, United States: USGS Reston. doi:10.5066/F78S4N29
- Gesch, D. B., Brock, J. C., Parrish, C. E., Rogers, J. N., and Wright, C. W. (2016). Introduction—special issue on advances in topobathymetric mapping, models, and applications. *J. Coast. Res.* SI (76), 1–3. doi:10.2112/SI76-001
- Herdendorf, C. E. (1982). Large lakes of the world. *J. Geol. Lakes. Res.* 8, 379–412. doi:10.1016/s0380-1330(82)71982-3
- Hess, L. L., Melack, J. M., Novo, E. M. L. M., Barbosa, C. C. F., and M. Gastil, M. (2012). LBA-ECO LC-07 JERS-1 SAR wetlands masks and land cover, amazon basin: 1995–1996. *Data Set*. doi:10.3334/ORNLDAAC/1079
- Jasinski, M. F., Stoll, J. D., Cook, W. B., Ondrusek, M., Stengel, E., and Brunt, K. (2016). Inland and near shore water profiles derived from the high altitude multiple altimeter beam experimental lidar (MABEL). *J. Coastal Research* 76 (sp1), 44–55. doi:10.2112/si76-005
- Jasinski, M., Stoll, J., Hancock, D., Robbins, J., Nattala, J., Morison, J., et al. (2019). *Algorithm theoretical basis Document (ATBD) for inland water data products, ATL13, version 002*. Greenbelt, MD: NASA Goddard Space Flight Center. doi:10.5067/3H94R271O0C
- Jasinski, M., Stoll, J., Hancock, D., Robbins, J., Nattala, J., Morison, J., et al. (2023). ICESat-2 algorithm theoretical basis document (ATBD) for along track inland surface water data, ATL13, version 6. ICESat-2 project. doi:10.5067/03JYGZ0758UL
- Jean-François, J., Cottam, A., Gorelick, N., and Belward, A. (2017). *Global surface water explorer dataset*. European Commission: Joint Research Centre JRC. Available online at: <http://data.europa.eu/89h/jrc-gsw-e-global-surface-water-explorer-v1>.
- Jet propulsion laboratory (2025). *DSWx product suite*. Available online at: <https://www.jpl.nasa.gov/go/opera/products/dswx-product-suite/>.
- Jones, J. W. (2019). Improved automated detection of subpixel-scale inundation—Revised dynamic surface water extent (DSWE) partial surface water tests. *Remote Sens.* 11 (4), 374. doi:10.3390/rs11040374
- Lehner, B., and Döll, P. (2004). Development and validation of a global database of lakes, reservoirs and wetlands. *J. Hydrology* 296 (1), 1–22. doi:10.1016/j.jhydrol.2004.03.028
- Lehner, B., and Grill, G. (2013). Global river hydrography and network routing: baseline data and new approaches to study the world's large river systems. *Hydrol. Process.* 27 (15), 2171–2186. doi:10.1002/hyp.9740
- Li, Y., Gao, H., Jasinski, M. F., Zhang, S., and Stoll, J. D. (2019). Deriving high-resolution reservoir bathymetry from ICESat-2 prototype photon-counting lidar and landsat imagery. *IEEE Trans. Geoscience Remote Sens.* 57 (10), 7883–7893. doi:10.1109/TGRS.2019.2917012
- Lvovich, M. I. (1970). *Proceedings of the reading symposium (world water balance)*, 2. Gentbrugge-Paris-Geneva: IASH-UNESCO-WMO, 401–415.
- Ma, Y., Xu, N., Liu, Z., Yang, B., Yang, F., Wang, X. H., et al. (2020). Satellite-derived bathymetry using the ICESat-2 lidar and Sentinel-2 imagery datasets. *Remote Sens. Environ.* 250, 112047. doi:10.1016/j.rse.2020.112047
- Markus, T., Neumann, T., Martino, A., Abdalati, W., Brunt, K. M., Csatho, B., et al. (2017). The ice, cloud, and land elevation Satellite-2 (ICESat-2): science requirements, concept, and implementation. *Remote Sens. Environ.* 190, 260–273. doi:10.1016/j.rse.2016.12.029
- Martino, A. J., Neumann, T., Kurtz, N., and MacLennan, D. (2019). ICESat-2 mission overview and early performance. *Proc. SPIE 11151, Sensors, Syst. Next-Generation Satell.* XXIII, 111510C. doi:10.1117/12.2534938
- Messenger, M. L., Lehner, B., Grill, G., Nedeva, I., and Schmitt, O. (2016). Estimating the volume and age of water stored in global lakes using a geo-statistical approach. *Nat. Commun.* 7, 13603. doi:10.1038/ncomms13603
- Neumann, T. A., Martino, A. J., Markus, T., Bae, S., Bock, M. R., Brenner, A. C., et al. (2019). The ice, cloud, and land elevation satellite - 2 mission: a global geolocated photon product derived from the advanced topographic laser altimeter system. *Remote Sens. Environ.* 233. doi:10.1016/j.rse.2019.111325
- Openstreetmap (2025). *Openstreetmap*. Available online at: <https://www.openstreetmap.org>.
- Pavelsky, T. M., and Smith, L. C. (2008). RivWidth: a software tool for the calculation of 00 from remotely sensed imagery. *IEEE Geoscience Remote Sens. Lett.* 5 (1), 70–73. doi:10.1109/LGRS.2007.908305
- Pavelsky, T. M., Durand, M., Andreadis, K., Beighley, E., Cauduro Dias de Paiva, R., Allen, G., et al. (2014). Assessing the potential global extent of SWOT river discharge observations. *J. Hydrology* 519, 1516–1525. doi:10.1016/j.jhydrol.2014.08.044
- Pickens, A. H., Hansen, M. C., Hancher, M., Stehman, S. V., Tyukavina, A., Potapov, P., et al. (2020). Mapping and sampling to characterize global inland water dynamics from 1999 to 2018 with full landsat time-series. *Remote Sens. Environ.* 243, 111792. doi:10.1016/j.rse.2020.111792
- Ricko, M., Carton, J. A., Charon, M., Birkett, C. M., and Jean-Francois Cretaux, J.-F. (2012). Intercomparison and validation of continental water level products derived from satellite radar altimetry. *J. Appl. Remote Sens.* 6 (1), 061710. doi:10.1117/1.JRS.6.061710
- Robinson, N., Regetz, J., and Guralnick, R. P. (2014). EarthEnv-DEM90: a nearly-global, void-free, multi-scale smoothed, 90m digital elevation model from fused ASTER and SRTM data. *ISPRS, J. Photogrammetry Remote Sens.* 87, 57–67. doi:10.1016/j.isprsjprs.2013.11.002
- Ryan, J. C., Smith, L. C., Cooley, S. W., Pitcher, L. H., and Pavelsky, T. M. (2020). Global characterization of inland water reservoirs using ICESat-2 altimetry and climate reanalysis. *Geophys. Res. Lett.* 47, e2020GL088543. doi:10.1029/2020gl088543
- Sayre, R., Noble, S., Hamann, S. L., Smith, R. A., Wright, D. J., Breyer, S. P., et al. (2019). New 30 meter resolution global shoreline vector and associated global islands database for the development of standardized ecological coastal units. *J. Oper. Oceanogr.* 12 (sup 2), S47–S56.
- Surface Water Ocean Topography (SWOT) (2024). SWOT level 2 water mask raster image data product, version C. Ver. C. PO.DAAC, CA, USA. doi:10.5067/SWOT-RASTER-2.0
- SWOTST (2023). IRIS: global river surface slopes from ICESat-2 and its contribution to SWOT. Available online at: [https://swotst.aviso.altimetry.fr/fileadmin/user\\_upload/SWOTST2023/posters\\_earlycareer/Scherer\\_IRIS\\_Poster\\_Early%20Career.pdf](https://swotst.aviso.altimetry.fr/fileadmin/user_upload/SWOTST2023/posters_earlycareer/Scherer_IRIS_Poster_Early%20Career.pdf).
- Tortini, R., Noujdina, N., Yeo, S., Ricko, M., Birkett, C. M., Khandelwal, A., et al. (2020). Satellite-based remote sensing data set of global surface water storage change from 1992 to 2018. *Earth Syst. Sci. Data* 12 (2), 1141–1151. doi:10.5194/essd-12-1141-2020

- U.S. Fish and Wildlife Service (2019). Coastal barrier resources system. Available online at: <https://www.fws.gov/cbra/maps/boundaries.html>.
- Verpoorter, C., Kutser, T., Seekell, D. A., and Tranvik, L. J. (2014). A global inventory of Lakes based on high-resolution satellite imagery. *Geophys. Res. Lett.* 41 (18), 6396–6402. doi:10.1002/2014gl060641
- Wang, J., Pottier, C., Cazals, C., Battude, M., Sheng, Y., Song, C., et al. (2023). The surface water and ocean topography mission (SWOT) prior lake database (PLD): lake mask and operational auxiliaries. doi:10.22541/au.170258987.72387777/v1
- Wessel, P., and Smith, W. H. F. (1996). A global, self-consistent, hierarchical, high-resolution shoreline database. *J. Geophys. Res.* 101 (B4), 8741–8743. doi:10.1029/96jb00104
- Winslow, L. A., Read, J. S., Hanson, P. C., and Stanley, E. H. (2014). Lake shoreline in the contiguous United States: quantity, distribution and sensitivity to observation resolution. *Freshw. Biol.* 59, 213–223. doi:10.1111/fwb.12258
- Wu, S., Cai, Y., Ke, C. Q., Xiao, Y., Li, H., He, Z., et al. (2025). SWOT mission enables high-precision and wide-coverage lake water levels monitoring on the Tibetan Plateau. *J. Hydrology Regional Stud.* 59, 102357. doi:10.1016/j.ejrh.2025.102357
- Yamazaki, D., Trigg, M. A., and Ikeshima, D. (2015). Development of a global 90 m water body map using multi-temporal Landsat images. *Remote Sens. Environ.* 171, 337–351. doi:10.1016/j.rse.2015.10.014
- Yamazaki, D., Ikeshima, D., Sosa, J., Bates, P. D., Allen, G. H., and Pavelsky, T. M. (2019). MERIT Hydro: a high-resolution global hydrography map based on latest topography datasets. *Water Resour. Res.* 55, 5053–5073. doi:10.1029/2019wr024873
- Yan, D., Li, M., Bi, W., Weng, B., Qin, T., Wang, J., et al. (2019). A data set of inland lake catchment boundaries for the Qiangtang Plateau. *Sci. Data* 6, 62. doi:10.1038/s41597-019-0066-x
- Yuan, C., Gong, P., and Bai, Y. (2020). Performance assessment of ICESat-2 laser altimeter data for water-level measurement over Lakes and reservoirs in China. *Remote Sens.* 12 (5), 770. doi:10.3390/rs12050770
- Zhang, G., Chen, W., and Xie, H. (2019). Tibetan Plateau's lake level and volume changes from NASA's ICESat/ICESat-2 and Landsat missions. *Geophys. Res. Lett.* 46 (22), 13107–13118. doi:10.1029/2019gl085032
- Zwally, H. J., Schutz, B., Abdalati, W., Abshire, J., Bentley, C., Brenner, A., et al. (2002). ICESat's laser measurements of polar ice, atmosphere, ocean, and land. *J. Geodyn.* 34 (Issues 3–4), 405–445. doi:10.1016/S0264-3707(02)00042-X